AIAA 80-0196R

Analysis of Multiple Weak Glancing Shock/Boundary-Layer Interactions

G. C. Paynter*
Boeing Military Airplane Company, Seattle, Wash.

An analysis is developed for the change in boundary-layer properties across a system of weak glancing shock/boundary-layer interactions. For a control volume about a given interaction, integral continuity, cross-stream momentum, and streamwise momentum equations are solved for the boundary-layer properties downstream of the interaction. Analytic functions are used to represent the velocity distributions in directions normal and tangential to the shock. A procedure is developed to generate these functions where the boundary layer has passed through one or more upstream interactions. Starting with the upstream interaction, the change in boundary-layer properties is computed sequentially. Computed results are presented for two pairs of interactions; in the first pair, the shocks are of the same family, and in the second pair, the shocks are of opposite family. Computed results are in qualitative agreement with available experimental observations.

Nomenclature

M = Mach number
n_{1i}, n_{2i} = first and second boundary-layer profile parameters in region i, respectively
p = static pressure
$\bar{p}$ = average static pressure on outer surface of the control volume
T = static temperature
T_t = total temperature
u = velocity component normal to the shock and parallel to the surface
$(u/u_e)_{i,j}$ = ratio of local to local external velocity in the ith region normal to the jth shock
w = velocity component tangential to the shock and parallel to the surface
$(w/w_e)_{i,j}$ = ratio of local to local external velocity in the ith region tangential to the jth shock
X = coordinate normal to the shock
y = coordinate normal to the surface
Z = coordinate tangential to the shock
α = inviscid flow deflection angle
γ = ratio of specific heats
δ = boundary-layer thickness
θ = shock angle
ρ = density

Subscripts

1 = upstream of a given shock
2 = downstream of a given shock
e = local value external to the boundary layer
i,j = properties in the ith region with vector directions relative to jth shock
I = value associated with the first shock of a shock system
II = value associated with the second shock of a system where the first and second shocks are of the same family
R = value associated with the second shock of a shock system where the second shock is of opposite family to the first shock

Presented as Paper 80-0196 at the AIAA 18th Aerospace Sciences Meeting, Pasadena, Calif., Jan. 14-16, 1980; submitted Jan. 28, 1980; revision received June 30, 1980.

*Senior Specialist Engineer. Associate Fellow AIAA.

Introduction

GLANCING shock/boundary-layer interactions (GSBLI) occur on the sideplates of supersonic two-dimensional mixed or external compression inlets[1] or on the wing surfaces of aircraft with highly swept wings in supersonic flight,[2] Fig. 1. These interactions arise when oblique shocks generated by changes in surface slope in the local flow direction interact with the boundary layer on a surface approximately normal to the shock generating surface (the sideplate of an inlet, for example). GSLBI are three-dimensional since the position of the shock on the surface changes in a cross-stream direction.

An analysis by Paynter[3] demonstrates that a control volume approach can be used to compute the change in boundary-layer properties across weak GSBLI where the boundary layer entering the interaction is fully developed and two dimensional. In a number of applications, systems of GSBLI will exist as shown in Fig. 1 for the sideplate of a two dimensional inlet. The boundary layer upstream of the first interaction on the sideplate is approximately two dimensional, but downstream of the first interaction, the boundary layer exhibits a cross flow induced by the first interaction which decays slowly with distance in the local stream direction.

The objective of this paper is to present an extension of the analysis of Ref. 3 to multiple weak GSBLI. A procedure was developed for generating analytic functions to represent the boundary-layer velocity distributions in directions normal and tangential to a given shock where the boundary layer has passed through one or more upstream interactions. The extended analysis was used to study the effects of various combinations of shock families and shock strengths on the development of an initially two-dimensional boundary layer. The extended analysis and the results of this study are presented herein.

Flow Model

Peake[4] defines a weak interaction as one in which there is no coalescence of the streamlines near the wall. The wall streamline pattern for a weak interaction is illustrated in Fig. 2.[5] With a fully developed two-dimensional turbulent boundary layer upstream of the shock interaction, the inviscid static pressure ratio across the shock, $P_2/P_1 \leq 1.5$ for a weak interaction.

The weak interaction resembles a two-dimensional flow through a normal shock in a plane normal to the shock and the surface.[6] The wall static pressure rise begins 5-10 boundary-layer thicknesses upstream of the inviscid shock location. In this initial interaction region, the wall static pressure rises rapidly and is similar to the "free interaction"

pressure rise characteristic of two-dimensional SBL interactions in a plane normal to the incident shock and the surface.[7] Most of the inviscid rise in static pressure has been achieved within about 10 boundary-layer thicknesses from the start of the pressure rise.

A strong traverse pressure gradient exists in the region of interaction.[8] This transverse pressure gradient produces a cross flow within the boundary layer in a process which is almost instantaneous in that it occurs at the physical location of the pressure gradient.[9] Downstream of the shock, the transverse pressure gradient disappears. The cross flow set up as the boundary layer passes through the region of interaction decays rather slowly as the boundary layer develops downstream of the shock.

The boundary-layer thickness downstream of the interaction is typically larger than that upstream. At a given distance normal to the wall within the interaction and within the boundary layer, the flow properties vary rapidly in a direction normal to the shock and are constant or vary slowly in a direction tangential to the shock.[9]

The flow model used to obtain a solution in the current study is based on experimental observations of the flow through the region of interaction and has the following features for a given interaction.

1) The flow is quasi-two-dimensional. The flow properties are assumed constant in a direction parallel to the incident shock.

2) The upstream boundary layer and inviscid flow properties are assumed known.

3) The downstream inviscid flow properties are known from oblique shock theory.

4) The static pressure downstream of the region of the interaction is constant normal to the wall.

5) The region of interaction is "short." This implies that entrainment is negligible and that viscous forces are negligible with respect to pressure forces.

6) The flow in the region of interaction is isoenergetic. This is not an essential assumption and merely avoids solving a separate energy equation for the interaction.

7) The turning of the local inviscid flow external to the boundary layer in a direction away from the wall is supersonic, and the turning of this flow back toward the wall is subsonic for the velocity components in a plane normal to the shock and the wall.

8) The velocity components normal and tangential to the shock both upstream and downstream of the region of interaction are well represented by analytic functions.

9) For multiple interactions, the boundary-layer redevelopment between SBLI is negligible. This is only approximately true when the SBLI are close together. This is not an essential assumption and eventually the boundary-layer redevelopment between shocks will be computed with a three-dimensional boundary-layer analysis.

Analysis and Solution Procedure

The analysis of Ref. 3 is extended to compute the change in boundary-layer properties across a system of weak GSBLI by taking control volumes about each interaction in the system as illustrated in Fig. 3 for two systems of interactions. In the first system, the shocks are of the same family. In the second, they are of opposite family. For a given shock interaction system, the change in boundary-layer properties is computed sequentially starting with the upstream interaction.

For a control volume about a given interaction, integral equations for continuity, momentum normal to the shock, and momentum tangential to the shock are solved, using the ideal gas and isoenergetic flow assumptions, for the boundary-layer properties downstream of the shock (given the properties entering the shock). For the control volume shown in Fig. 4, integral continuity, x-momentum, and z-momentum

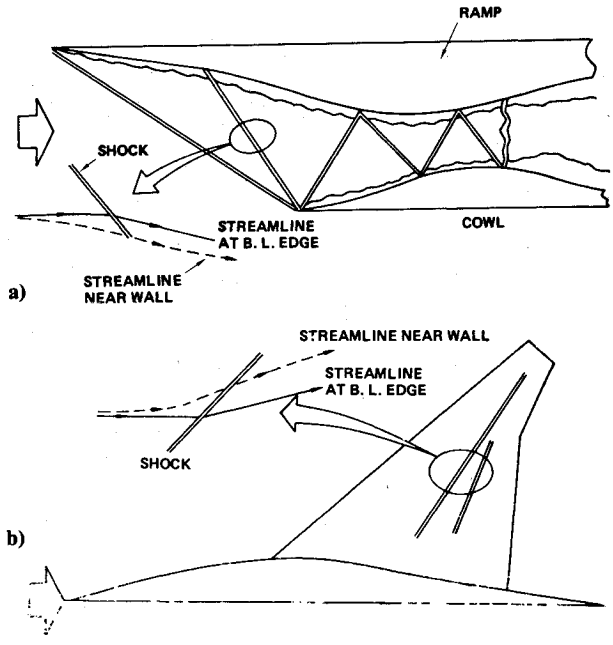

Fig. 1 a) Two-dimensional inlet shock pattern and b) fuselage induced shocks on the wing of a supersonic aircraft.

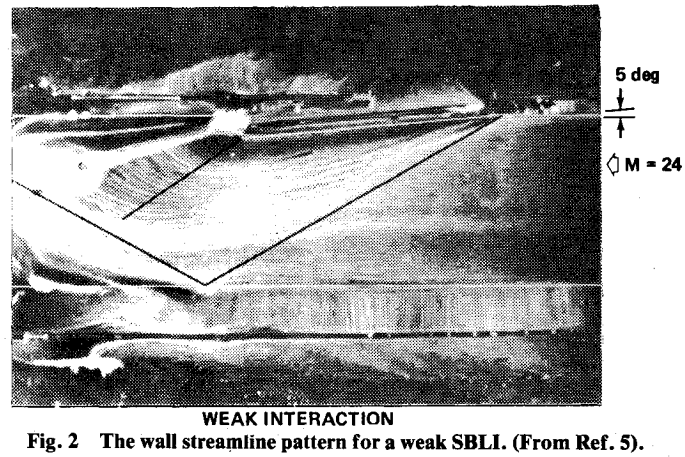

Fig. 2 The wall streamline pattern for a weak SBLI. (From Ref. 5).

equations may be written as follows:

Continuity

$$\int_0^\delta \rho u dy \Big|_1 = \int_0^\delta \rho u dy \Big|_2 \tag{1}$$

x Momentum

$$p_1\delta_1 + \bar{p}(\delta_2 - \delta_1) - p_2\delta_2 = \int_0^\delta \rho u^2 dy \Big|_2 - \int_0^\delta \rho u^2 dy \Big|_1 \tag{2}$$

z Momentum

$$\int_0^\delta w\rho u dy \Big|_1 = \int_0^\delta w\rho u dy \Big|_2 \tag{3}$$

The term $\bar{p}$ that appears in Eq. (2) is the average pressure acting on the upper surface of the control volume. If one assumes that the turning away from the wall is supersonic and the turning back toward the wall is subsonic in terms of the velocity components in a plane normal to the shock and the

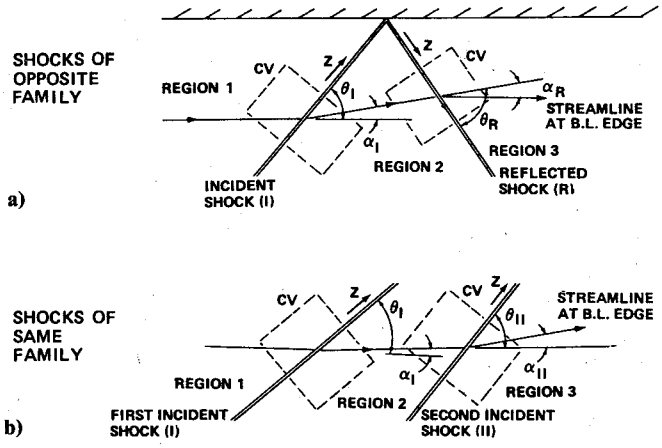

Fig. 3 Control volume (CV) geometries for multiple interactions.

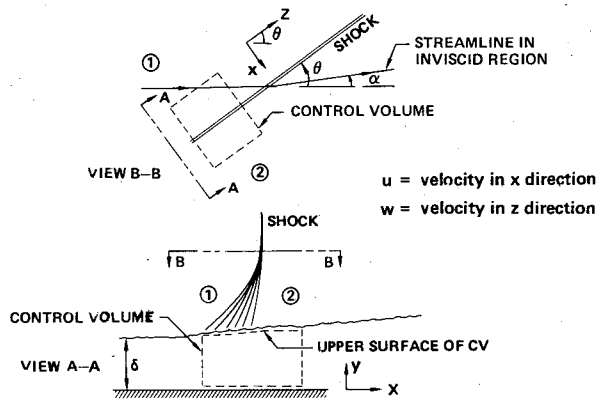

Fig. 4 The control volume (CV).

wall, $\bar{p}/p_1$ can be approximated by the expression,

$$\frac{\bar{p}}{p} = 0.67\frac{p_2}{p_1} + 0.33\{[1+(\gamma-1)M_1^2\sin^2\theta/2] / [1+(\gamma-1)/2]\}^{\gamma/(\gamma-1)} \tag{4}$$

This expression implies that the supersonic compression occurs without any change in thickness to a state at which the Mach number external to the boundary layer, in a plane normal to the shock, is equal to one. The remainder of the compression is assumed to occur such that shape of the curve of static pressure as a function of x, nondimensionalized by the interaction length, is parabolic. Combining Eqs. (1) and (2) yields

$$\frac{p_2}{p_1}\frac{M_2}{M_1}\frac{\sqrt{1+\left(\frac{\gamma-1}{2}\right)M_2^2}\sin(\theta-\alpha)\int_0^1 \frac{\rho u}{\rho_e u_e}\,d(y/\delta)\Big|_2}{\sqrt{1+\left(\frac{\gamma-1}{2}\right)M_1^2}\sin(\theta)\int_0^1 \frac{\rho u}{\rho_e u_e}\,d(y/\delta)\Big|_1}$$

$$-\frac{\left\{\frac{p_2}{p_1}-\frac{\bar{p}}{p_1}+\frac{p_2}{p_1}[\gamma M_2^2\sin^2(\theta-\alpha)]\int_0^1 \frac{\rho u^2}{\rho_e u_e^2}\,d(y/\delta)\Big|_2\right\}}{\left\{1-\frac{\bar{p}}{p_1}+\gamma M_1^2\sin^2\theta\int_0^1 \frac{\rho u^2}{\rho_e u_e^2}\,d(y/\delta)\Big|_1\right\}} = 0 \tag{5}$$

Combining Eqs. (1) and (3) yields

$$\left(\frac{1+\left(\frac{\gamma-1}{2}\right)M_2^2}{1+\left(\frac{\gamma-1}{2}\right)M_1^2}\right)^{1/2}\frac{\int_0^1 \frac{\rho u}{\rho_e u_e}\,d(y/\delta)\Big|_2}{\int_0^1 \frac{\rho u}{\rho_e u_e}\,d(y/\delta)\Big|_1}$$

$$-\left\{\frac{M_2\cos(\theta-\alpha)\int_0^1 \frac{\rho u w}{\rho_e u_e w_e}\,d(y/\delta)\Big|_2}{M_1\cos\theta\int_0^1 \frac{\rho u w}{\rho_e u_e w_e}\,d(y/\delta)\Big|_1}\right\} = 0 \tag{6}$$

The ideal gas and isoenergetic flow assumptions can be used to obtain an expression for the ratio of the local density to the local freestream density.

$$\frac{\rho}{\rho_e} = [1-[(\gamma-1)/2]M_e^2(T_e/T_t)] \div \left\{\frac{1-[(\gamma-1)/2][(u/u_e)^2u_e^2+(w/w_e)^2w_e^2](T_e/T_t)}{\gamma RT_e}\right\} \tag{7}$$

If one assumes that, downstream of the shock, the normal and tangential velocity components u/u_e and w/w_e are representable by two parameter analytic functions, Eqs. (4) and (7) can be substituted into Eqs. (5) and (6) to yield two equations that can be solved for the profile parameters. Once the profile parameters are known, Eq. (1) can be solved for the change in boundary-layer thickness across the region of interaction.

Velocity Profile Representations

The general analytic representations for the normal and tangential velocity components upstream and downstream of a given shock interaction within a system are developed through consideration of a shock reflection system and a system consisting of two shocks of the same family both shown in Fig. 3. Starting with the shock reflection system, note that the boundary layer upstream of the incident shock is assumed to be two dimensional and have a power law velocity distribution. Using the control volume analysis of Ref. 3, the velocity components normal and tangential to the incident shock in region 2 are known and are represented by power laws with exponents n_{12} and n_{22}. The velocity components normal and tangential to the reflected shock can be expressed in terms of the velocity components normal and tangential to incident shock by a resolution of the velocity vectors relative to the incident shock into components relative to the reflected shock in region 2;

$$\frac{u_{2R}}{u_{2R_e}} = -\frac{\cos(\theta_1+\theta_R-\alpha_I)\sin(\theta_1-\alpha_I)}{\sin\theta_R}(y/\delta)^{1/n_{12}} + \frac{\sin(\theta_1+\theta_R-\alpha_I)\cos(\theta_1-\alpha_I)}{\sin\theta_R}(y/\delta)^{1/n_{22}} \tag{8}$$

$$\frac{w_{2R}}{w_{2R_e}} = \frac{\sin(\theta_1+\theta_R-\alpha_I)\sin(\theta_1-\alpha_I)}{\cos\theta_R}(y/\delta)^{1/n_{12}} + \frac{\cos(\theta_1+\theta_R-\alpha_I)\cos(\theta_1-\alpha_I)}{\cos\theta_R}(y/\delta)^{1/n_{22}} \tag{9}$$

where u_{2R}/u_{2R_e} and w_{2R}/w_{2R_e} are the ratios of the local velocity to the local external velocity in directions normal and tangential to the reflected shock in region 2.

By inspection of Eqs. (8) and (9), one observes that the right side of each equation is composed of two terms which are summed to give the velocity ratio normal or tangential to the reflected shock. Each of the four terms is the product of a "geometry" part, a function of the inviscid shock and turning angles and a profile part, a function of y/δ. For a GSBLI with a two dimensional boundary-layer upstream of the region of interaction, the form of the analytic functions representing the boundary-layer in the normal and tangential directions remains unchanged across the interaction. If this is assumed

to be true for the reflected shock interaction as well, the forms of the velocity components in directions normal and tangential to the reflected shock in region 3 can be written as follows.

$$\frac{u_{3R}}{u_{3R_e}} = -\frac{\cos(\theta_I+\theta_R-\alpha_I)\sin(\theta_I+\alpha_R-\alpha_I)}{\sin(\theta_R-\alpha_R)}(y/\delta)^{1/n_{13}} + \frac{\sin(\theta_I+\theta_R-\alpha_I)\cos(\theta_I+\alpha_R-\alpha_I)}{\sin(\theta_R-\alpha_R)}(y/\delta)^{1/n_{23}} \quad (10)$$

$$\frac{w_{3R}}{w_{3R_e}} = \frac{\sin(\theta_I+\theta_R-\alpha_I)\sin(\theta_I+\alpha_R-\alpha_I)}{\cos(\theta_R-\alpha_R)}(y/\delta)^{1/n_{13}} + \frac{\cos(\theta_I+\theta_R-\alpha_I)\cos(\theta_I+\alpha_R-\alpha_I)}{\cos(\theta_R-\alpha_R)}(y/\delta)^{1/n_{23}} \quad (11)$$

Note that u_{3R}/u_{3R_e} and w_{3R}/w_{3R_e} are the ratios of local to local external velocity in directions normal and tangential to the reflected shock in region 3. n_{13} and n_{23} are the unknown profile parameters that are determined through solution of Eqs. (4-7).

Following a similar development for a shock system consisting of two shocks of the same family, expressions can be written[10] for the ratios of local velocity to local external velocity components in directions normal and tangential to the second shock of the system in regions 2 and 3. As for the reflected shock system, each term of the velocity component expressions in regions 2 and 3 for the second shock can be divided into a geometry part and a profile part. For the second shock of the system, n_{13} and n_{23} are again the unknown profile parameters which are to be determined through solution of Eqs. (4-7).

If one were to consider an additional shock, downstream of either the reflected shock system or the system of two incident shocks, this process of developing the analytic functions to represent the normal and tangential velocity profile components upstream and downstream of this shock could be continued in a manner similar to that just outlined. The functions which represent the velocity components normal and tangential to the ith -1 shock in a system of interactions will, in general, have the following form in the ith region (just upstream of the ith shock).

$$\left.\frac{u}{u_e}\right|_{i,i-1} = f_{i-1}(y/\delta)^{1/n_{1,i}} + g_{i-1}(y/\delta)^{1/n_{2,i}} \quad (12)$$

$$\left.\frac{w}{w_e}\right|_{i,i-1} = h_{i-1}(y/\delta)^{1/n_{1,i}} + k_{i-1}(y/\delta)^{1/n_{2,i}} \quad (13)$$

The functions f_{i-1}, g_{i-1}, h_{i-1}, and k_{i-1} are the geometry parts of the velocity functions with respect to the ith -1 shock.

Consider a system of shocks in which the ith shock of the system is of opposite family to the ith -1 shock. The velocity component ratios normal and tangential to the ith shock in the ith region (the ith region is just upstream of the ith shock) can be written as follows.

$$\left.\frac{u}{u_e}\right|_{i,i} = -\frac{\cos(\theta_{i-1}+\theta_i-\alpha_{i-1})\sin(\theta_{i-1}-\alpha_{i-1})}{\sin\theta_i}\left.\frac{u}{u_e}\right|_{i,i-1} + \frac{\sin(\theta_{i-1}+\theta_i-\alpha_{i-1})\cos(\theta_{i-1}-\alpha_{i-1})}{\sin\theta_i}\left.\frac{w}{w_e}\right|_{i,i-1} \quad (14)$$

$$\left.\frac{w}{w_e}\right|_{i,i} = \frac{\sin(\theta_{i-1}+\theta_i-\alpha_{i-1})\sin(\theta_{i-1}-\alpha_{i-1})}{\cos\theta_i}\left.\frac{u}{u_e}\right|_{i,i-1} + \frac{\cos(\theta_{i-1}+\theta_i-\alpha_{i-1})\cos(\theta_{i-1}-\alpha_{i-1})}{\cos\theta_i}\left.\frac{w}{w_e}\right|_{i,i-1} \quad (15)$$

Substituting Eqs. (12) and (13) into Eqs. (14) and (15), Eqs. (14) and (15) can be rewritten,

$$\left.\frac{u}{u_e}\right|_{i,i} = (Xf_{i-1}+Yh_{i-1})(y/\delta)^{1/n_{1,i}} + (Xg_{i-1}+Yk_{i-1})(y/\delta)^{1/n_{2,i}} \quad (14')$$

$$\left.\frac{w}{w_e}\right|_{i,i} = (Wf_{i-1}+Zh_{i-1})(y/\delta)^{1/n_{1,i}} + (Wg_{i-1}+Zk_{i-1})(y/\delta)^{1/n_{2,i}} \quad (15')$$

where

$$X = -\frac{\cos(\theta_{i-1}+\theta_i-\alpha_{i-1})\sin(\theta_{i-1}-\alpha_{i-1})}{\sin\theta_i}$$

$$Y = \frac{\sin(\theta_{i-1}+\theta_i-\alpha_{i-1})\cos(\theta_{i-1}-\alpha_{i-1})}{\sin\theta_i}$$

$$W = \frac{\sin(\theta_{i-1}+\theta_i-\alpha_{i-1})\sin(\theta_{i-1}-\alpha_{i-1})}{\cos\theta_i}$$

$$Z = \frac{\cos(\theta_{i-1}+\theta_i-\alpha_{i-1})\cos(\theta_{i-1}-\alpha_{i-1})}{\cos\theta_i}$$

The velocity component ratios normal and tangential to the ith shock in the ith $+1$ region (just downstream of the ith shock) can be written as follows.

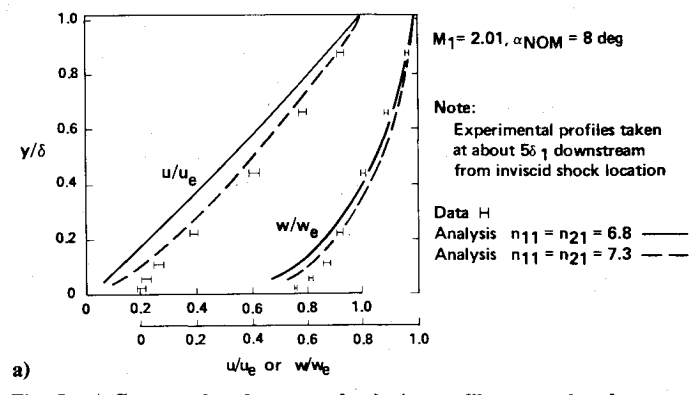

a)

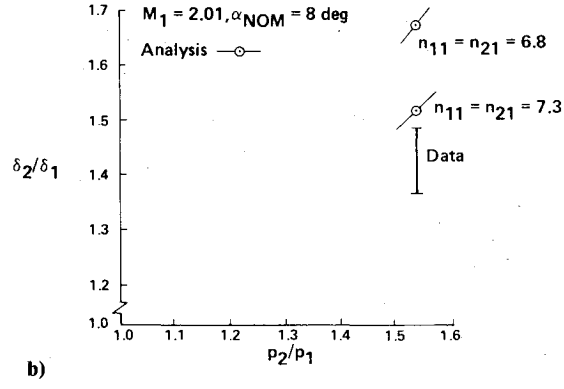

b)

Fig. 5 a) Computed and measured velocity profiles normal and tangential to the shock and b) computed and measured change in δ across the interaction.

$$\left.\frac{u}{u_e}\right|_{i+1,i} = -\frac{\cos(\theta_{i-1}+\theta_i-\alpha_{i-1})\sin(\theta_{i-1}+\alpha_i-\alpha_{i-1})}{\sin(\theta_i-\alpha_i)}\left.\frac{u}{u_e}\right|_{i+1,i-1} + \frac{\sin(\theta_{i-1}+\theta_i-\alpha_{i-1})\cos(\theta_{i-1}+\alpha_i-\alpha_{i-1})}{\sin(\theta_i-\alpha_i)}\left.\frac{w}{w_e}\right|_{i+1,i-1} \tag{16}$$

$$\left.\frac{w}{w_e}\right|_{i+1,i} = \frac{\sin(\theta_{i-1}+\theta_i-\alpha_{i-1})\sin(\theta_{i-1}+\alpha_i-\alpha_{i-1})}{\cos(\theta_i-\alpha_i)}\left.\frac{u}{u_e}\right|_{i+1,i-1} + \frac{\cos(\theta_{i-1}+\theta_i-\alpha_{i-1})\cos(\theta_{i-1}+\alpha_i-\alpha_{i-1})}{\cos(\theta_i-\alpha_i)}\left.\frac{w}{w_e}\right|_{i+1,i-1} \tag{17}$$

The velocity ratios $u/u_e|_{i+1,i-1}$ and $w/w_e|_{i+1,i-1}$ have the same form as $u/u_e|_{i,i-1}$ and $w/w_e|_{i,i-1}$ except that the "profile" parts have changed across the ith shock.

$$\left.\frac{u}{u_e}\right|_{i+1,i-1} = f_{i-1}(y/\delta)^{1/n_{1,i+1}} + g_{i-1}(y/\delta)^{1/n_{2,i+1}} \tag{18}$$

$$\left.\frac{w}{w_e}\right|_{i+1,i-1} = h_{i-1}(y/\delta)^{1/n_{1,i+1}} + k_{i-1}(y/\delta)^{1/n_{2,i+1}} \tag{19}$$

Substituting Eqs. (18) and (19) into Eqs. (16) and (17), Eqs. (16) and (17) can be rewritten as follows.

$$\left.\frac{u}{u_e}\right|_{i+1,i} = [pf_{i-1}+qh_{i-1}](y/\delta)^{1/n_{1,i+1}} + [pg_{i-1}+qk_{i-1}](y/\delta)^{1/n_{2,i+1}} \tag{16'}$$

$$\left.\frac{w}{w_e}\right|_{i+1,i} = [Rf_{i-1}+th_{i-1}](y/\delta)^{1/n_{1,i+1}} + [Rg_{i-1}+tk_{i-1}](y/\delta)^{1/n_{2,i+1}} \tag{17'}$$

Note that Eqs. (16′) and (17′) have the same form as Eqs. (12) and (13). If we rewrite Eqs. (16′) and (17′) in this form,

$$\left.\frac{u}{u_e}\right|_{i+1,i} = f_i(y/\delta)^{1/n_{1,i+1}} + g_i(y/\delta)^{1/n_{2,i+1}} \tag{16''}$$

$$\left.\frac{w}{w_e}\right|_{i+1,i} = h_i(y/\delta)^{1/n_{1,i+1}} + k_i(y/\delta)^{1/n_{2,i+1}} \tag{17''}$$

then the geometry portions of the profiles downstream of the ith and ith -1 shocks are related as follows.

$$f_i = pf_{i-1}+qh_{i-1} \qquad h_i = Rf_{i-1}+th_{i-1}$$

$$g_i = pg_{i-1}+qk_{i-1} \qquad k_i = Rg_{i-1}+tk_{i-1}$$

where

$$p = -\frac{\cos(\theta_{i-1}+\theta_i-\alpha_{i-1})\sin(\theta_{i-1}+\alpha_i-\alpha_{i-1})}{\sin(\theta_i-\alpha_i)}$$

$$R = \frac{\sin(\theta_{i-1}+\theta_i-\alpha_{i-1})\sin(\theta_{i-1}+\alpha_i-\alpha_{i-1})}{\cos(\theta_i-\alpha_i)}$$

$$q = \frac{\sin(\theta_{i-1}+\theta_i-\alpha_{i-1})\cos(\theta_{i-1}+\alpha_i-\alpha_{i-1})}{\sin(\theta_i-\alpha_i)}$$

$$t = \frac{\cos(\theta_{i-1}+\theta_i-\alpha_{i-1})\cos(\theta_{i-1}+\alpha_i-\alpha_{i-1})}{\cos(\theta_i-\alpha_i)}$$

For a system of shock interactions in which the ith and ith -1 shocks of the system are of the same family, the development for the normal and tangential velocity component ratios upstream and downstream of the ith shock is similar to that when the shocks are of opposite family except that,

$$X = \frac{\cos(\theta_i+\alpha_{i-1}-\theta_{i-1})\sin(\theta_{i-1}-\alpha_{i-1})}{\sin\theta_i}$$

$$Y = \frac{\sin(\theta_i+\alpha_{i-1}-\theta_{i-1})\cos(\theta_{i-1}-\alpha_{i-1})}{\sin\theta_i}$$

$$W = -\frac{\sin(\theta_i+\alpha_{i-1}-\theta_{i-1})\sin(\theta_{i-1}-\alpha_{i-1})}{\cos\theta_i}$$

$$Z = \frac{\cos(\theta_i+\alpha_{i-1}-\theta_{i-1})\cos(\theta_{i-1}-\alpha_{i-1})}{\cos\theta_i}$$

and

$$p = \frac{\cos(\theta_i-\theta_{i-1}+\alpha_{i-1})\sin(\theta_{i-1}-\alpha_{i-1}-\alpha_i)}{\sin(\theta_i-\alpha_i)}$$

$$R = -\frac{\sin(\theta_i-\theta_{i-1}+\alpha_{i-1})\sin(\theta_{i-1}-\alpha_{i-1}-\alpha_i)}{\cos(\theta_i-\alpha_i)}$$

$$q = \frac{\sin(\theta_i-\theta_{i-1}+\alpha_{i-1})\cos(\theta_{i-1}-\alpha_{i-1}-\alpha_i)}{\sin(\theta_i-\alpha_i)}$$

$$t = \frac{\cos(\theta_i-\theta_{i-1}+\alpha_{i-1})\cos(\theta_{i-1}-\alpha_{i-1}-\alpha_i)}{\cos(\theta_i-\alpha_i)}$$

$u/u_e|_{i+1,i}$ and $w/w_e|_{i+1,i}$ are the ratios of the local velocity to the local external velocity in the directions normal and tangential to the ith shock in the ith + 1 region. The unknown profile parameters, $n_{1,i+1}$ and $n_{2,i+1}$ are determined through solution of Eqs. (4-7). The profile parameters, $n_{1,i}$ and $n_{2,i}$, and the geometry information are known for a given interaction.

The general velocity profile representations for the normal and tangential velocity components with respect to a given shock could be developed from boundary-layer velocity profile representations other than the power law. For example, the compressible law-of-the-wall law-of-the-wake velocity profile of Ref. 11 could be used as the basis for the development just given. Use of a representation such as that of Ref. 11 should improve the accuracy of the representation in the boundary layer near the wall. The algebra required to develop the general profile expressions would be substantially more complicated and, since all of the profile parameters would occur in each velocity profile expression, the machine time required to achieve a solution would increase somewhat.

Computer Program

Equations (4-7) are solved iteratively with a Newton-Raphson scheme for the profile parameters downstream of a given shock. The integrals appearing in the equations are evaluated with a numerical integration procedure. The change in boundary-layer thickness across the interaction is found from Eq. (1). The run time to compute the change in boundary-layer properties across a given interaction is 0.3-0.5 CPU seconds on the CDC Cyber 175 computer.

Results and Discussion

Results of the calculation procedure[3] are compared with experimental data by Peake[4] in Fig. 5 for an interaction flow at $M_1 = 2.01$ and a nominal deflection angle of 8 deg. The nominal static pressure rise across the interaction was 1.54 and $Re_{\delta_1} = 1.5\times10^5$. The boundary-layer upstream of the interaction was two dimensional and well represented by a power law with an exponent between 6.8 and 7.3. The predicted normal and tangential velocity profile components

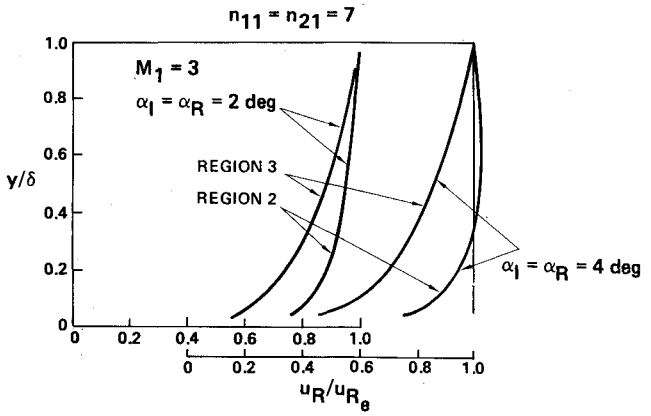

Fig. 6 Distortion of the normal velocity component through the reflected shock.

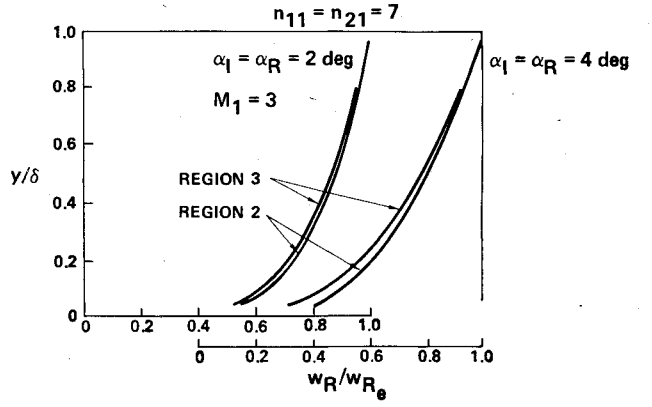

Fig. 7 Distortion of the tangential velocity component through the reflected shock.

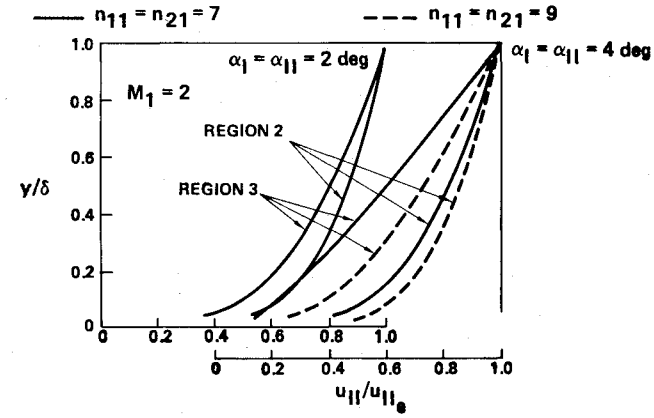

Fig. 8 Distortion of the normal velocity component through the second shock.

downstream of the shock are compared with test data in Fig. 5a. The predicted change in boundary-layer thickness across the interaction is given in Fig. 5b. The solid lines in Figs. 5a and b are the results downstream of the interaction assuming an upstream power law exponent of 6.8; the dotted lines show the results for an upstream power law exponent of 7.3. The procedure for arriving at the power law exponents for the Peake data is discussed in Ref. 3. These results and similar results for a 4 deg deflection interaction at $M_I = 3$ from Ref. 9, also presented in Ref. 3, illustrate that the analysis of Ref. 3 does predict the correct trend for the distortion of the velocity components normal and tangential to the shock across the shock and the correct trend for the change in boundary-layer thickness across the shock.

The extended analysis was used to compute the change in boundary-layer properties across two types of shock interaction systems. The first type of system is a shock reflection from a wall where the shocks are of opposite family; the second system consists of two shocks of the same family.

The predicted distortion of the boundary-layer velocity component normal to the reflected shock through the reflected shock of the first system is shown in Fig. 6 for 2 and 4 deg shock deflection angles at $M_I = 3$. The region 2 profiles are just upstream of the reflected shock interaction and the region 3 profiles are just downstream. As expected, the analysis predicts that the normal velocity profile becomes less full through a given interaction and that the profile distortion increases with shock strength. The analysis predicts that an increase in the power law exponent in region 1 from 7 to 9 reduces the profile distortion.[10]

The predicted distortion of the boundary-layer velocity component tangential to the reflected shock for the first system is shown in Fig. 7 for the same Mach number and shock deflection angles considered for the normal velocity component. The tangential velocity component becomes less full through a given interaction. Again, the predicted profile distortion increases with shock strength and decreases with an increase in the upstream power law exponent. The predicted distortion of the tangential velocity component through the reflected shock is less than that for the normal velocity component.

The predicted distortion of the boundary-layer velocity component normal to the second shock of a two shock system where the shocks are of the same family is shown in Fig. 8 for shock deflection angles of 2 and 4 deg at $M_I = 2$. As for the shock reflection system, the profile distortion increases with shock strength and decreases with an increase in the upstream power law exponent.

The predicted distortion of the boundary-layer velocity component tangential to the second shock of the shock system where the two shocks are of the same family is shown in Fig. 9 for the same Mach number and shock strengths as for the normal velocity component. As for the shock reflection system, the predicted profile distortion increases with increasing shock strength and decreases with an increase in the upstream power law exponent. Again, the predicted distortion of the tangential velocity component is less than that for the normal velocity component. The predicted change in boundary-layer thickness across the second shock of both shock systems is as follows. The ratio of downstream to upstream boundary-layer thickness increases with increasing shock deflection angle and decreases with an increase in the upstream power law exponent.

No measurements are known to exist for the development of the boundary-layer velocity field through a multiple shock system. One might ask, since velocity field measurements have not been reported, why a simple analytic function, such as a power law, is not used to represent the velocity components normal and tangential to a given shock within a system of interactions. One might further ask what evidence supports the use of the rather more complex analytic profile representations as described by Eqs. (14-17).

Note the unusual shape of the velocity component normal to the reflected shock in region 2 of a reflected shock interaction system at $M_I = 3$ and with $\alpha_I = \alpha_R = 4$ deg as shown in Fig. 6. This profile results from a resolution of the velocity field downstream of the incident shock into components normal and tangential to the reflected shock. The only assumptions are that the analysis of Ref. 3 correctly predicts the velocity field downstream of the incident shock and that the boundary-layer redevelopment between the incident and reflected shocks is negligible. While it may be possible to find simple two or three parameter analytic functions that will represent the range of velocity profile distributions shown in Figs. 6-9, it is obvious that the standard representations would be inadequate.

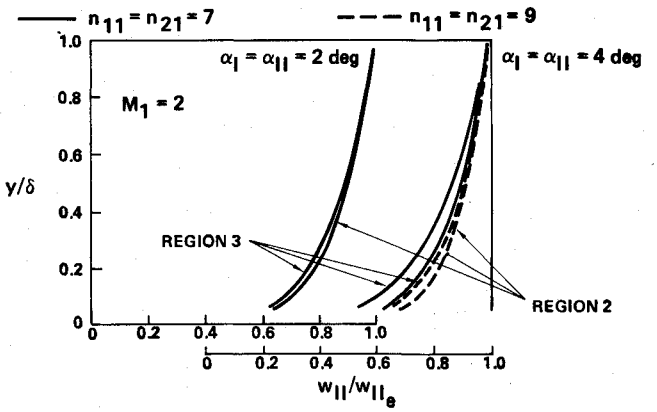

Fig. 9 Distortion of the tangential velocity component through the second shock.

The only direct physical observations of a multiple GSBLI system are reported by Dickman.[5] Photographs of oil flow visualization studies by Dickman for shock reflection interactions at Mach 2.4 over a range of shock strengths show a flow disturbance in the corner region between the sideplate and the tunnel wall opposite the shock generating surface just downstream of the shock reflection. The size of the disturbed corner flow region appears to increase with increasing shock strength. As described next, this qualitative effect is predicted by the analysis.

Based on past experience with two- and three-dimensional boundary-layer flows, the predicted behavior of the boundary layer through a multiple shock interaction system does appear reasonable. One would expect the largest response of the velocity field to occur in the direction with the largest adverse pressure gradient which is, in this case, a direction normal to the shock. One can show, for the tangential velocity component, that the tangential component is constant on a stream surface through the interaction. This implies that the tangential velocity profile is merely stretched as the boundary layer changes thickness across an interaction.

With reference to the computed changes in the normal and tangential velocity components across the two shock systems considered here, note that the normal velocity component becomes much less full across the interaction and that the tangential component, while it becomes less full, distorts much less than the normal velocity component. A direct validation of the analysis and the velocity profile representations must await the availability of suitable test data; however, computed results from the present analysis do appear to be consistent with prior experience as to the behavior of a boundary layer subject to a strong adverse pressure gradient.

The extended analysis of the present study was used to investigate the net effect of a shock reflection interaction on the corner flow downstream of the interaction.[10] It was found that a shock reflection interaction induces a cross flow into the corner in the region downstream of the shock reflection. Once established, the cross flow into the corner should persist a substantial distance downstream of the interaction and disappear only gradually with the viscous redevelopment of the boundary layer. The predicted cross flow increases rapidly with increasing shock strength. This is consistent with the observations of Dickman.[5]

The effect of mass removal or bleed on the boundary-layer velocity distribution is to make the profiles "more full" or to increase the power law exponent of a power law fit to the velocity profile downstream of a bleed band. An increase in the power law exponent of the velocity profile upstream of a shock reflection from 7 to 9 substantially reduces the cross flow into the corner and should therefore reduce the flow disturbance emanating from the corner.

Conclusions

The analysis of Ref. 3 was extended to predict the change in boundary-layer properties across a system of multiple weak glancing shock interactions with shocks of both families present. The extension required the development of analytic velocity profile representations for the boundary-layer velocity components normal and tangential to a given shock within the system. The procedure for generating these functions was generalized for an arbitrary number and combination of shock interactions. While a detailed validation of the analysis must await the availability of detailed flow survey measurements, the analysis is consistent with prior experience as to the response of a boundary-layer flow subjected to a strong adverse pressure gradient. The analysis predicts a cross flow into the corner region for a shock reflection interaction. This is in qualitative agreement with experimental observations that a disturbance originates in the corner region downstream of a shock reflection interaction that increases in size with increasing shock strength.

Computed results were presented to show the effects of upstream Mach number, upstream boundary-layer properties, and shock strengths on the boundary-layer properties downstream of the second shock of two shock interaction systems. In the first system, the shocks were of opposite family. In the second system, they were of the same family. The computed results indicate that a boundary layer developing through a shock pair of opposite family can withstand a much larger static pressure rise before the onset of a strong interaction than a boundary layer developing through a shock pair of the same family.

References

[1] *Proceedings of the 1977 NASA Lewis Inlet Workshop,* 1977.

[2] Kulfan, R. M. and Sigalla, A., "Real Flow Limitations in Supersonic Airplane Design," *Journal of Aircraft,* Vol. 16, Oct. 1979, pp. 645-658.

[3] Paynter, G. C., "Analysis of Weak Glancing Shock Boundary Layer Interactions," AIAA Paper 79-0144, Jan. 1979; also, *Journal of Aircraft,* Vol. 17, March 1980, pp. 160-166.

[4] Peake, D. J., "Three-Dimensional Swept Shock/Turbulent Boundary-Layer Separations With Control by Air Injection," National Research Council Canada, Aero. Rept. LR-592, July 1976.

[5] Dickman, C. C., "Glancing Interaction With a Turbulent Boundary Layer," AFOSR-76-3006, July 1977.

[6] Green, J. E., "Interactions Between Shock Waves and Turbulent Boundary Layers," *Progress in Aerospace Sciences,* Vol. 11, Pergamon Press, Oxford, 1970, pp. 235-340.

[7] McCabe, A., "The Three-Dimensional Interaction of a Shock Wave With a Turbulent Boundary Layer," *Aeronautical Quarterly,* Aug. 1966, pp. 231-252.

[8] Oskam, B., Vas, I. E., and Bogdonoff, S. M., "Mach 3.0 Oblique Shock Wave/Turbulent Boundary Layer Interactions in Three-Dimensions," AIAA Paper 76-336, 1976.

[9] Oskam, B., Vas. I. E., and Bogdonoff, S. M., "An Exploratory Study of a Three-Dimensional Shock Wave Boundary Layer Interaction at Mach 3," Princeton Univ., Princeton, N. J., Rept. 1227, May 1975.

[10] Paynter, G. C., "Analysis of Multiple Weak Glancing Shock Boundary Layer Interaction," AIAA Paper 80-0196, Jan. 1980.

[11] Mathews, D. C., Childs, M. E., and Paynter, G. C., "Use of Coles' Universal Wake Function for Compressible Turbulent Boundary Layers," *Journal of Aircraft,* Vol. 7, March-April 1970, pp. 137-140.